Experiments in Coherent Change Detection for Synthetic Aperture Sonar

Daniel D. Sternlicht,[a] J. Kent Harbaugh,[b] Matthew A. Nelson[b]

[a] Naval Surface Warfare Center, Panama City Division
110 Vernon Ave
Panama City FL 32407 USA

[b] Applied Signal Technology, Inc.
20101 Hamilton Ave, Suite 150
Torrance CA 90502 USA

***Abstract*-Automatic Change Detection (ACD) compares new and stored terrain images for alerting to changes occurring over time. ACD techniques, long used in airborne radar applications, are just beginning to be applied to sidescan sonar. In Coherent Change Detection (CCD) the cross-correlation of multi-temporal complex data collected from coherent imaging sonars detects changes in the transduced amplitudes and phase of image pixels which, under the right conditions, can be used to detect new objects or disturbances on the seafloor. Synthetic aperture sonars (SAS) produce range-independent, fine resolution seafloor images. With centimetric resolution demonstrated out to hundreds of meters, these coherent systems can classify small manmade objects at long ranges, and should be suitable for CCD.**

This paper describes experiments testing CCD with data from synthetic aperture sonars mounted on autonomous undersea vehicles and actively navigated tow bodies. A noncoherent example carried out with data collected from an AUV-mounted SAS demonstrates the utility of correlation-based automatic change detection. CCD tests were carried out with repeat pass data collected using a SAS mounted on a dynamically controlled tow vehicle. While simple image pair co-registration procedures failed to provide sufficient coherence in the overall scene required for CCD, preliminary tests of image warping techniques used for airborne radar applications show promise of transitioning successfully into the SAS signal processing chain.

I. Introduction

Since the terrorist attacks of September 2001, concern on how best to protect ports and water-ways continues to grow. As techniques for inspecting cargo containers and surveilling small craft and swimmers become operational, countering the threat of mines or improvised explosive devices (IED) placed in sea lanes is beginning to be addressed. Effective countermeasures must combine gathering and acting upon intelligence that a mining event is about to occur, periodic mapping of ingress/egress routes to catalog and classify newly appearing objects, and effective coordination of explosive ordnance disposal capabilities.

Harbors and high volume traffic lanes typically have large quantities of debris resembling potential targets that can easily saturate conventional sonar detection approaches. Thus automatic change detection (ACD) techniques pioneered in airborne radar, comparing new and stored terrain images to alert changes over time, are being evaluated for use in bottom surveys that utilize seafloor mapping sonars. In this application, bottom imagery from periodic surveys is used to maintain a database of historical (benign) objects and to detect the appearance of new potential threats.

This paper describes preliminary experiments of applying coherent change detection (CCD) techniques for detecting the presence of manmade objects newly laid in estuary environments. The systems considered are the EdgeTech 4400 synthetic aperture sonar (SAS) deployed on a HUGIN 1000 autonomous undersea vehicle (AUV) and an Applied Signal Technology (AST) SAS deployed on a MacArtney FOCUS-2 Remotely Operated Tow Vehicle (ROTV).

Sections II and III of this paper describe approaches for automatic change detection and introduces CCD. Section IV provides an example of noncoherent change detection using the AUV-mounted SAS. Section V describes a coherent change detection experiment using the ROTV-mounted SAS. Section VI discusses the findings to date and charts future directions.

II. Background

Change detection methods are categorized based on their unsupervised or supervised nature. The first category is correlation-based and compares multi-temporal image data. The second category typically is feature-based and involves matching algorithms. In airborne radar applications, correlation-based ACD was developed first, feature-based ACD came later, and the two approaches are being fused in the synthetic aperture radar (SAR) research community [1]. In sonar, due to challenges in navigation (trajectory control and accurate georegistration), the complexity of the propagation environment, and the radiometric inconsistencies of conventional sidescan sonars, feature-based approaches were developed first (e.g. the methods of Gendron *et al.* [2]). Only in recent years, with the advent of synthetic aperture sonars and actively navigated platforms, have correlation-based methods been shown to be feasible [3].

0-933957-38-1

Synthetic aperture sonars produce range-independent, fine resolution seafloor images. With centimetric resolution demonstrated out to hundreds of meters, these systems are well suited for classifying small manmade objects. When mounted on actively navigated platforms capable of accurately repeating survey tracks, radiometric inconsistencies between old and new data are minimized. For SAS systems, incoherent and coherent correlation-based ACD approaches are possible, where the former identifies changes in mean backscatter power of a scene, and the latter identifies changes in both the amplitude and phase of the transduced imagery that arise in the interval between collections. For radar it is generally accepted that processing the complex imagery is necessary for detecting changes on the scale of small man-made objects [4], and it is likely that robust correlation-based ACD for sonar systems will follow suit. As conventional sidescan sonars exhibit resolution that degrades with range and are typically limited to creation of backscatter amplitude images, they are less suitable for small-scale correlation-based ACD—thus explaining early adaption of feature-based ACD for sidescan systems.

III. Correlation-Based Change Detection

The correlation-based change detection process is outlined in Fig. 1. Baseline and repeat-pass images are geographically co-registered onto a single grid. A correlation map between the two images is computed, where it follows that changes between the two scenes produce areas of low correlation. These "decorrelation" contacts are detected, and features corresponding to these areas are used by an automatic target recognition module (ATR) or operator to classify the contacts as of interest or not.

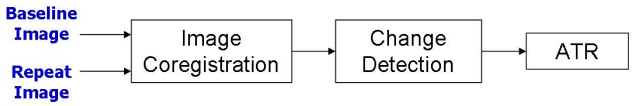

Fig. 1. General Block Diagram For Correlation-based Automatic Change Detection

We explored two methods of image co-registration. Common to each approach is an initial gross alignment: where sensor altitude is used to transform slant range to ground range, and latitude, longitude and heading outputs from the navigation suite are used to locate each pixel. For AUV and ROTV SAS data, fine-scale co-registration was carried out using the methods of parcel cross-correlation and iterative trajectory refinement, respectively, which are described in the following sections.

IV. Experiment with AUV-mounted SAS

To test the feasibility of applying correlation-based change detection to SAS imagery, repeat passes over a relatively featureless bottom were conducted with a 120-kHz, 10-cm resolution EdgeTech 4400 SAS mounted on a HUGIN 1000 AUV (Fig. 2) in 2004. The baseline pass image is shown in Fig. 3a. The image for a repeat pass conducted two hours later is shown in Fig. 3b, into which a simulated contact was injected at range of 35 m. The simulated contact consists of a 50 cm×50 cm patch, for which the pixel magnitudes were scaled by a factor of four. The images were converted to a common grid and subsequently divided into 2.5 m×2.5 m parcels. Parcels were cross-correlated between scenes to find the two-dimensional translations that maximize the correlation. From these translations, a "rubber-sheet" warp map was constructed and used to adjust the images to minimize geo-registration errors.

The inter-scene correlation map of the warped images is shown in Fig. 3c, where it is observed that the majority of the area exhibits a correlation of greater than 0.7, and the injected contact causes a significant local drop in correlation (0.6). A detector based on a statistical model of the correlation distribution automatically determines an optimal threshold segmenting the contact from the rest of the map (Fig. 3d). Note that the equally bright real contact in both images has been rejected and the results reveal only changes between the scenes.

Fig. 2. HUGIN 1000 with EdgeTech 4400 SAS

The procedure described for Fig. 3 was carried out solely with the amplitude images. Correlation with amplitude is more robust against image co-registration errors and a non-static environment than complex coherence. Utilizing the amplitude images, this example shows that correlation-based change detection can be successfully carried out when an ideal reflector is injected into a tractable data set—in this case, two well-matched tracks (range offset on the order of 1 m) and a stationary environment.

V. Experiment with ROTV-mounted SAS

To test coherent change detection with real objects, a 175-kHz, 2.5-cm resolution AST SAS mounted on a FOCUS-2 ROTV (Fig. 4 and [6]) was used to conduct repeat survey tracks in an estuary environment. The FOCUS-2 is a dynamically controlled tow vehicle with a guidance suite that integrates inertial navigation and ultrashort baseline systems (INS, USBL) with a Doppler velocity log (DVL), allowing accurate following of pre-programmed tracks, semi-independent of ship motion.

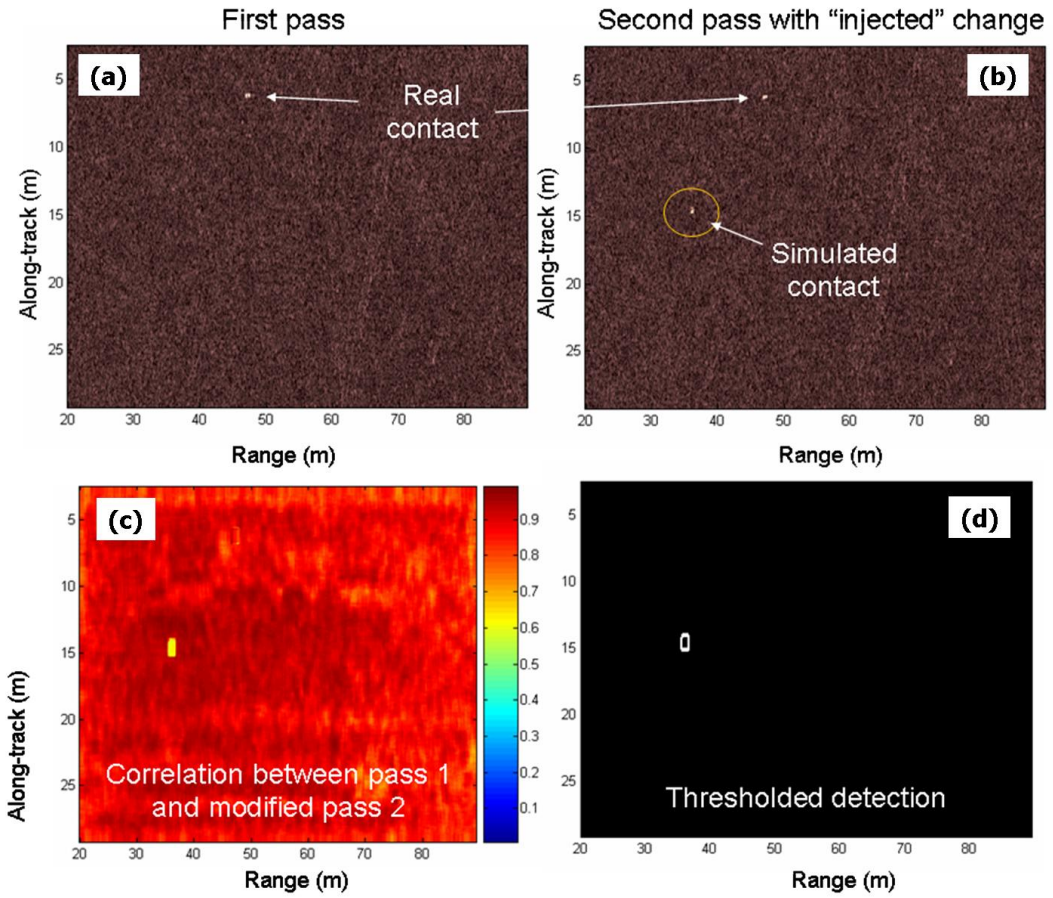

Fig. 3. Change Detection Example: Image Warping Using Parcel Cross-Correlation. Images are from port array.

After completion of the baseline track, a triangular pyramid target, constructed of 1.2-m rebar sides and draped in chicken wire (Fig. 5), was deployed and resurveyed 90 minutes later. The trajectory of the repeat pass was executed within 4 meters of the original—the target positioned approximately 50 m to starboard. Co-registered image segments of the baseline and repeat pass are shown in Fig. 6; where the newly laid target is clearly visible in the center of panel (b).

Fig. 4. ProSAS Surveyor: AST SAS and MacArtney ROTV

Fig. 5. Proxy Target: Triangular Pyramid

For image co-registration, we initially tried the parcel cross-correlation method described in Sec. IV. The inter-scene amplitude-only correlation plot (Fig. 7) resulting from this operation shows that while the majority of the area correlates above 0.65, roughly one third of the area has correlation values of less than 0.65—a baseline co-registration insufficiently robust to support correlation-based change detection (whether coherent or noncoherent).

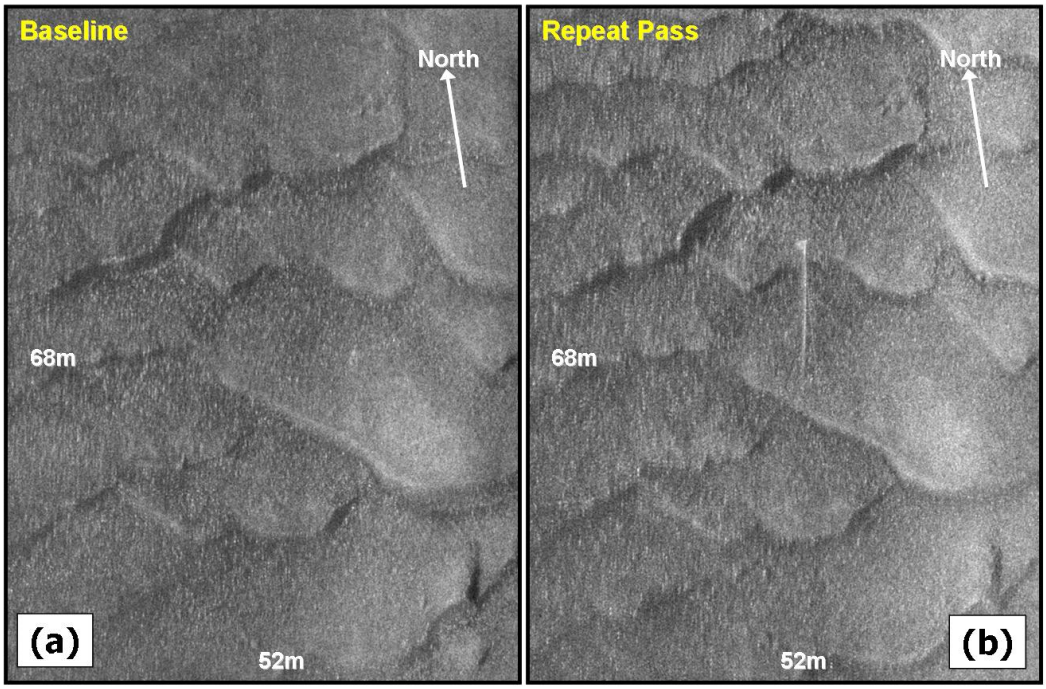

Fig. 6. Baseline (a) and repeat pass (b) images after co-registration by trajectory refinement warping. The vehicle track is northerly and images are from the starboard array. The target and its float lines are visible in the center of panel (b).

Since the parcel cross-correlation warping uses only translations, distortions caused by trajectory rotations or twisting are not corrected. We expect a generalized warp map that includes both translation and rotation will produce correlation maps sufficient for automated coherent change detection and will explore these procedures in future work.

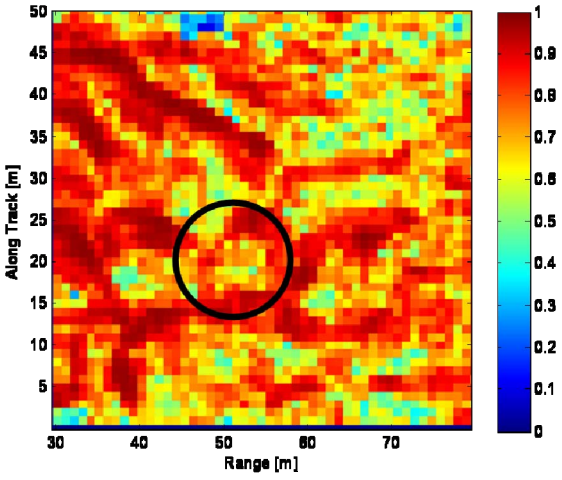

Fig. 7. Correlation maps between amplitude images of the baseline pass and repeat passes after application of the parcel cross-correlation warping method. The circle designates target location.

A second co-registration method being explored involves image warping based on iterative trajectory refinement, developed by AST and User Systems Inc. for synthetic aperture radar CCD. A significant portion of the co-registration error is hypothesized to be due to deviations between the recorded navigation of the sensor and its actual trajectory [7]. Accordingly, the co-registration method attempts to correctly adjust the sensor trajectory used to map the scene. Parcels of high inter-scene correlation are used as tie-points, around which sensor trajectories are iteratively modified to maximize overall inter-scene coherence. The technique is in the process of being adapted to SAS image formation, and currently precludes key SAS processing steps like Redundant Phase Center motion compensation [8]. Preliminary results are explored here.

The co-registered baseline and repeat pass images resulting from the trajectory refinement warping method are shown in Fig. 6. These two scenes are, to the eye, very well correlated—with the exception of the added target in the repeat pass, and some contrast in shadow depth resulting from the original trajectory differential. Fig. 8a shows the magnitude of the complex correlation map, and Fig 8b shows the phase difference map—calculated by subtracting the complex phases of the images. The overall correlation is modest; however, some regions in the image show excellent correlation. These are manifest by bright spots in the correlation map and corresponding interference fringes in the phase difference map—regions that serve as primary tie points for the algorithm. The existence of these features indicates that the data is suitable for CCD and that the fundamentals of the co-registration algorithm are working due to sufficient spectral overlap between the passes [9]. We anticipate that significant increases in inter-scene coherence will

result from integration of the trajectory refinement algorithm into the SAS processor.

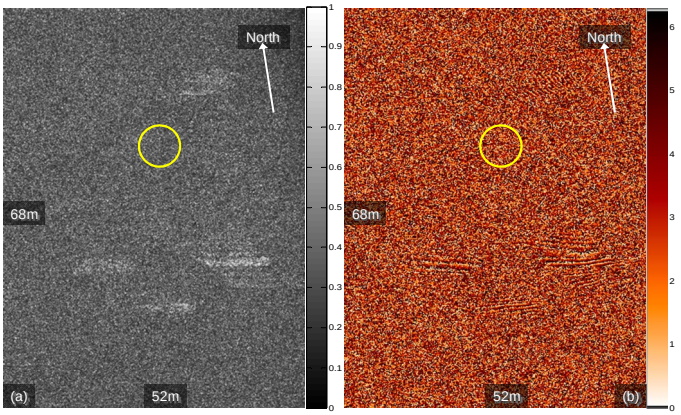

Fig. 8. Preliminary results of trajectory refinement warp technique: (a) Magnitude of complex correlation map. Bright areas are regions of high inter-scene coherence; (b) Phase difference map. The circles designate target location.

VI. Discussion

Using a data set collected with an AUV-mounted 120-kHz, 10-cm resolution SAS, a noncoherent example demonstrated the utility of correlation-based automatic change detection for alerting to the presence of objects newly introduced to the seafloor. This data set was well-suited for correlation-based ACD, in that it exhibited the fine, range-independent resolution of a SAS system, and was characterized by a 1-m track repetition, stationary environment, and an idealized, synthetically inserted target. Image co-registration was achieved with a two-stage process of initial gross alignment, followed by parcel cross-correlation warping. However, short SAS frame lengths introduced phase discontinuities that make computation of the complex inter-scene correlation more difficult. For this initial study, we have not yet implemented the adjustments necessary to find complex correlation across frames.

To take advantage of the increased sensitivity of coherent processing that SAS affords, a repeat pass experiment was conducted using an ROTV-mounted 175-kHz, 2.5-cm resolution SAS, and deployment of a real target. SAS frames of extended lengths were generated; however, the parcel cross-correlation method was insufficient to adequately co-register the two images, as it successfully did for the AUV example. This result is likely a function of trajectory and wavelength. The change in imaging geometry caused by the 4-meter lateral offset of the ROTV passes likely contributed to loss of inter-scene coherence—an offset that will be reduced with more experience programming and operating the ROTV for SAS surveys. Spatial coherence also degrades with reduction in acoustic wavelength—where the wavelength of the ROTV SAS (0.86 cm) is thirty percent shorter than that of the AUV SAS (1.25 cm). (Other factors can include environmental complexity, temporal stationarity, system noise, and data processing imperfections.) Initial testing of a trajectory refinement warping technique developed for SAR CCD produced results indicating that proper integration into the SAS processor will result in co-registration adequate for SAS CCD.

Future work includes integration of SAR co-registration methods into the SAS processor, fine tuning vehicle settings for more accurate track repetition in both AUV and active towfish operations, and exploration of lower acoustic frequencies and more suitable imaging geometries in order to reduce baseline decorrelation.

References

[1] P. Gamba, F. Dell'Acqua, G. Lisini, "Change Detection of Multitemporal SAR Data in Urban Areas Combining Feature-Based Techniques," IEEE Transactions on GeoScience and Remote Sensing, Vol. 44, No. 10, pp. 2820-2827, October 2006.

[2] M. Gendron, M. Lohrenz, G. Layne, J. Ioup, "Automatic Change Detection and Classification (ACDC) System," Proceedings of the Sixth International Symposium on Technology and the Mine Problem, Naval Postgraduate School, Monterey, CA. May 9-13, 2004.

[3] D. Sternlicht, M. Nelson, K. Harbaugh, J. Pesaturo, "Change Detection Techniques for Rapid Localization of Maritime IEDs," NDIA Joint Undersea Warfare, 10 September 2008.

[4] M. Preiss and N. J. S. Stacey, "Coherent Change Detection: Theoretical Description and Experimental Results," DSTO-TR-1851, August, 2006.

[5] D. Sternlicht and J. F. Pesaturo. *Synthetic Aperture Sonar: Frontiers in Underwater Imaging*, Sea Technology, 45(11), pp. 27-32. November 2004.

[6] Applied Signal Technology and MacArtney Underwater Technology, "ROTV Sonar," UT^2 Society for Underwater Technology, pp. 36-38, August 2008.

[7] H. Zebker, C. Werner, P. Rosen and S. Hensley, "Accuracy of Topographic Maps Derived from ERS-1 interferometric Radar," IEEE Trans. Geoscience and Remote Sensing, vol. 32, no. 4, pp. 823-836, July 1994.

[8] A. Putney, E. Chang, R. Chatham, D. Marx, M. Nelson, L. K. Warman, "Synthetic Aperture Sonar – the Modern Method of Underwater Remote Sensing," IEEE Aerospace 2001 Conference Proceedings, March 20.

[9] C.V. Jakowatz, Jr, D.E. Wahl, P.H. Eichel, D.C. Ghiglia and P.A. Thompson, "Spotlight-Mode Synthetic Aperture Radar: a Signal Processing Approach." Boston, MA: Kluwer, 1996.